

# Study of the pyroelectric profile in BTS piezoceramics by the single frequency thermal square wave method

O. Malyshkina<sup>a,\*</sup>, A. Movchikova<sup>a</sup>, R. Steinhausen<sup>b</sup>, H.T. Langhammer<sup>b</sup>, H. Beige<sup>b</sup>

<sup>a</sup> Tver State University, Sadoviy per. 35, 170002 Tver, Russia

<sup>b</sup> Martin-Luther-University Halle-Wittenberg, Friedemann-Bach-Platz 6, 06108 Halle, Germany

Available online 3 June 2009

## Abstract

Lead-free BaTi<sub>1-x</sub>Sn<sub>x</sub>O<sub>3</sub> (BTS) piezoceramics finding its use in actuators and microsensors was studied with the aid of the thermal square wave method (TSWM). Functionally graded BTS with tin concentration of  $0.075 \leq x \leq 0.15$  varying over the sample thickness were investigated. The samples were fabricated by sintering of the bi-, tri- and tetramorph green bodies. The results were compared with the pyroelectric profiles of BTS samples without tin gradient with  $x = 0.075, 0.10, 0.125$  and  $0.15$ .

© 2009 Elsevier Ltd. All rights reserved.

**Keywords:** B. Non-destructive evaluation; C. Ferroelectric properties; D. BaTiO<sub>3</sub> and titanates; E. Actuators; Pyroelectric properties

## 1. Introduction

The method of heat waves is widely applied in the studies of polarization distribution over the thickness of ferroelectric crystals. One of the main techniques of the investigation of polarization profile, the laser intensity modulation method (LIMM),<sup>1–6</sup> is based on the use of sinusoidal heat flux modulation. In LIMM a solution of the integral Fredholm equation of the first kind is required for the reconstruction of polarization distribution from the pyrocurrent frequency dependence. This method is used for modulation frequencies of 5 Hz–20 MHz, so it is limited to the study of films or surface layers of bulk samples.

In the present work we propose a single frequency thermal square wave method (TSWM) for the determination of the thickness distribution of pyrocoefficient based on the pyroresponse analysis under the condition of rectangular heat flux modulation. In the TSWM method the coordinate dependence of the effective pyroelectric coefficient is determined from the time dependence of the pyroelectric response. With the use of digital methods of signal processing the TSWM method makes it possible to study the polarization distribution in bulk materials.

The TSWM method was used for the study of BaTi<sub>1-x</sub>Sn<sub>x</sub>O<sub>3</sub> (BTS) ceramics. This novel type of lead-free material is widely used in piezoelectric actuators and microsensors. Ceramics

with continuously varying chemical composition after poling acquires an inhomogeneous distribution of dielectric and piezoelectric properties. Such functional gradient materials are especially suitable for bending actuators, e.g., in bimorph layered systems. Among the advantages of these materials are low internal stresses, low production costs and the possibility to design lead-free systems.

## 2. Theory

It is convenient to represent the square heat wave by the Fourier expansion.<sup>7,8</sup> Formally the wave is presented by a complex function. However, only the real part of this function has the physical meaning so it should be used in calculations.<sup>8–10</sup>

In the case of square heat flux modulation the heating rate is constant during the light pulse time and the phase shift between the heat flux and pyroelectric response is absent.<sup>11</sup> So the change of thermal wave characteristics inside the sample is taken into account by including the temperature wave velocity<sup>8</sup> into the design equations. The pyroelectric signal is registered in the real time regime, i.e., the value of  $U(t)$  is fixed. Consider one half of the period (the time during which the heat flux is applied to the crystal). Inasmuch as the heat wave propagation velocity is finite, the wave penetration distance for the time  $t$ <sup>12</sup> is:

$$x = ut = 2t\sqrt{\alpha\pi f}, \quad (1)$$

where  $\alpha$  is the thermal diffusion coefficient, and  $f$  is the heat flux modulation frequency.

\* Corresponding author.

E-mail address: [Olga.Malyshkina@mail.ru](mailto:Olga.Malyshkina@mail.ru) (O. Malyshkina).

In this case it is possible to interpret  $U(t)$  as  $U(x)$ . As a result the  $\gamma(x)$  may be found from the equation

$$I = S\gamma \frac{\partial \Theta}{\partial t}, \quad (2)$$

where  $S$  is the illuminated sample area,  $\gamma$  is the pyrocoefficient, and  $\partial \Theta / \partial t$  is the rate of temperature changes. In the case of  $\omega > 2\alpha/d^2$ , using a compact form for the temperature change distribution proposed by H.I. Zajos,<sup>7</sup> the pyrocoefficient is expressed as<sup>13</sup>:

$$\gamma(x) = \frac{U(t)kT}{4R_{OA}S\beta_0W_0} \operatorname{Re} \left\{ \left( \sum_{n=1}^{\infty} \frac{\sin^2(n\omega\tau/2)}{n\omega\tau/2} \frac{i}{\varphi_n^2 2t\sqrt{\alpha\pi f}} (1 - \exp[\varphi_n(-x)]) \right)^{-1} \right\}, \quad (3)$$

where  $\gamma(x)$  is the effective pyroelectric coefficient of a layer with a thickness  $x$ ,  $R_{OA}$  is the resistance of the operational amplifier,  $T = 1/f$  is the period,  $\varphi_n = (1 + i)\sqrt{n\omega/2\alpha}$ ,  $\tau$  is the light duration,  $d$  is the sample thickness,  $W_0$  is the heat flux power density,  $\beta_0$  is the coefficient of heat absorption,  $k$  is the thermal conductivity coefficient.

### 3. Experimental

In the TSWM measurement, the on–off cycle of an IR-photodiode ( $\lambda = 930\text{--}960$  nm) was controlled by a wave function generator connected in series with a power amplifier. The pyroelectric current was converted to voltage by an operational amplifier OP297 with conversion coefficient of 250 V/ $\mu$ A in the bandwidth of 1000 Hz. Signal sampling was performed by a 12-bit analog–digital converter LA-70M4 at a sampling frequency of 13 kHz.

BaTi<sub>1-x</sub>Sn<sub>x</sub>O<sub>3</sub> ceramics were measured at a frequency 0.1 Hz. BaTi<sub>1-x</sub>Sn<sub>x</sub>O<sub>3</sub> functional ceramics with a tin gradient of  $0.075 \leq x \leq 0.15$  were synthesized by successive pressing of the granulated powders with different Sn content and sintering the green bodies for 1 h at 1400 °C under an uniaxial pressure of about 1 kPa. Bimorph (Z), trimorph (D) and tetramorph (V) samples were composed of layers with  $x = 0.075 + 0.15$ ,  $0.075 + 0.1 + 0.15$ , and  $0.075 + 0.1 + 0.125 + 0.15$ , respectively. Homogeneous samples with  $x = 0.075$ , 0.1, 0.125 and 0.15 were also prepared. Al electrodes were evaporated onto both sides of the samples. Poling was performed at 20 kV/cm by applying a positive DC voltage to the top electrode.

The pyroelectric coefficient was measured for both sides of the samples. After that the pyroelectric profiles were calculated according to Eq. (3). The obtained curves were linked together at the middle of the samples.

The coefficient of thermal diffusion,  $\alpha$ , required for the pyroelectric profile calculation was determined independently for each sample of the given tin concentration. The measurements were performed at  $T = 25$  °C. At this temperature the samples with  $x = 0.075$  and 0.10 are in the ferroelectric phase ( $\alpha = 2 \times 10^{-7}$  m<sup>2</sup>/c), while those with  $x = 0.125$  and 0.15 are near the Curie point and are characterized by  $\alpha = 2.5 \times 10^{-7}$  m<sup>2</sup>/c.

Table 1

The temperatures of the permittivity maximum for different BTS samples.

Samples	$T_{\max \varepsilon}$ (°C)
Z, D, V	45
BTS7.5	72
BTS10	59
BTS12.5	34
BTS15	18

### 4. Results

According to Ref.<sup>14</sup> the introduction of tin decreases the Curie region of BTS ceramics, so the temperature dependence of the dielectric permittivity was measured to define the ferroelectric and paraelectric temperature regions of all the samples under study. As expected, it was observed that tin indeed decreases the temperature interval of the Curie region of the homogeneous samples (Table 1), in contrast to gradient ones, for which the temperature of the dielectric permittivity maximum was independent of the number of layers (Table 1). The temperature dependences of the pyroelectric coefficient  $\gamma$  measured by the dynamic method show that the  $\gamma$  maximum is 5–10° lower than the maximum of the dielectric permittivity.

The room temperature ( $T = 25$  °C) polarization profiles of BTS ceramics with tin gradients are presented in Fig. 1. The left sides of the graphs correspond to the negative ends of the polarization vector right sides correspond to the positive ends. It is seen from the presented profiles that the polarization distribution is asymmetric – a layer with inverse polarization exists on the positive side of the sample, while a layer with higher polarization values is registered on the opposite ( $-P_s$ ) side.

The main role in the formation of this asymmetry belongs to the direction of the composition gradient, depending on the sample side for which the temperature of measurement corresponds to the temperature of either the ferroelectric phase constituents or to the paraelectric ones. The layer with inverse polarization exists near the surface corresponding to the BTS15 composition. Comparison of the pyroelectric profiles of multilayer BTS ceramics with different number of layers shows that the polarization is maximal in the central part of a sample when 2/3 parts of it is composed of BTS7.5 and BTS10 being in their ferroelectric phase at the temperature of measurement. The minimal polarization value is observed in the middle of the four-layer sample.

Shown in Fig. 2 (curves 1) are the pyroelectric profiles of homogeneous samples of BTS ceramics measured at 27 °C. For these samples the difference in the polarization distribution curves is due to the fact that they have different Curie temperatures.

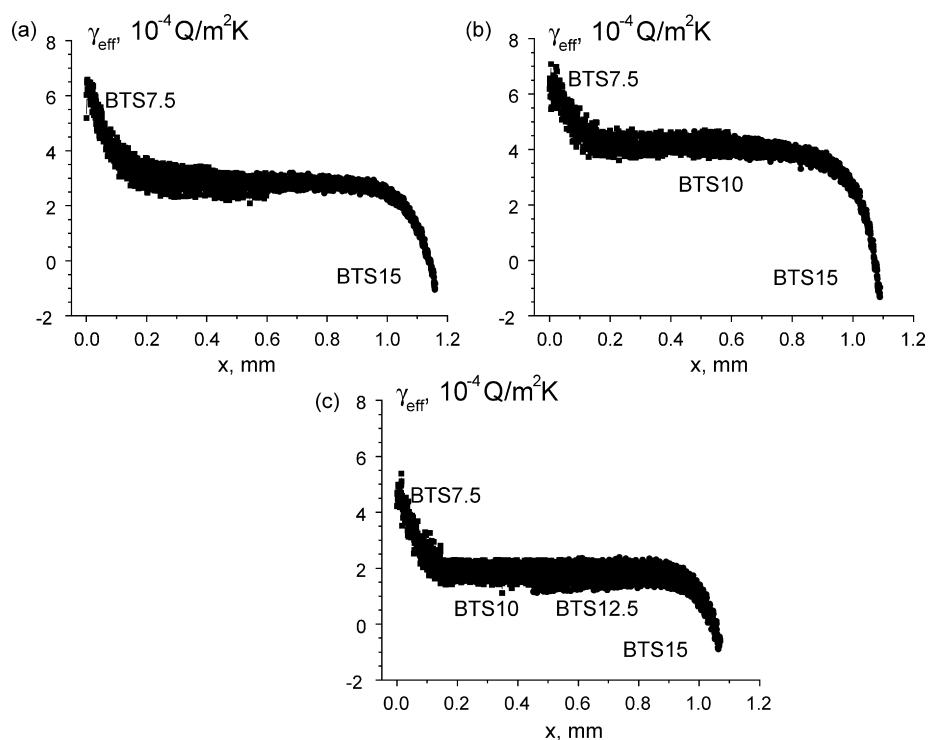


Fig. 1. Pyroelectric coefficient profile of a bimorph (a), trimorph (b) and tetramorph (c) BTS samples.

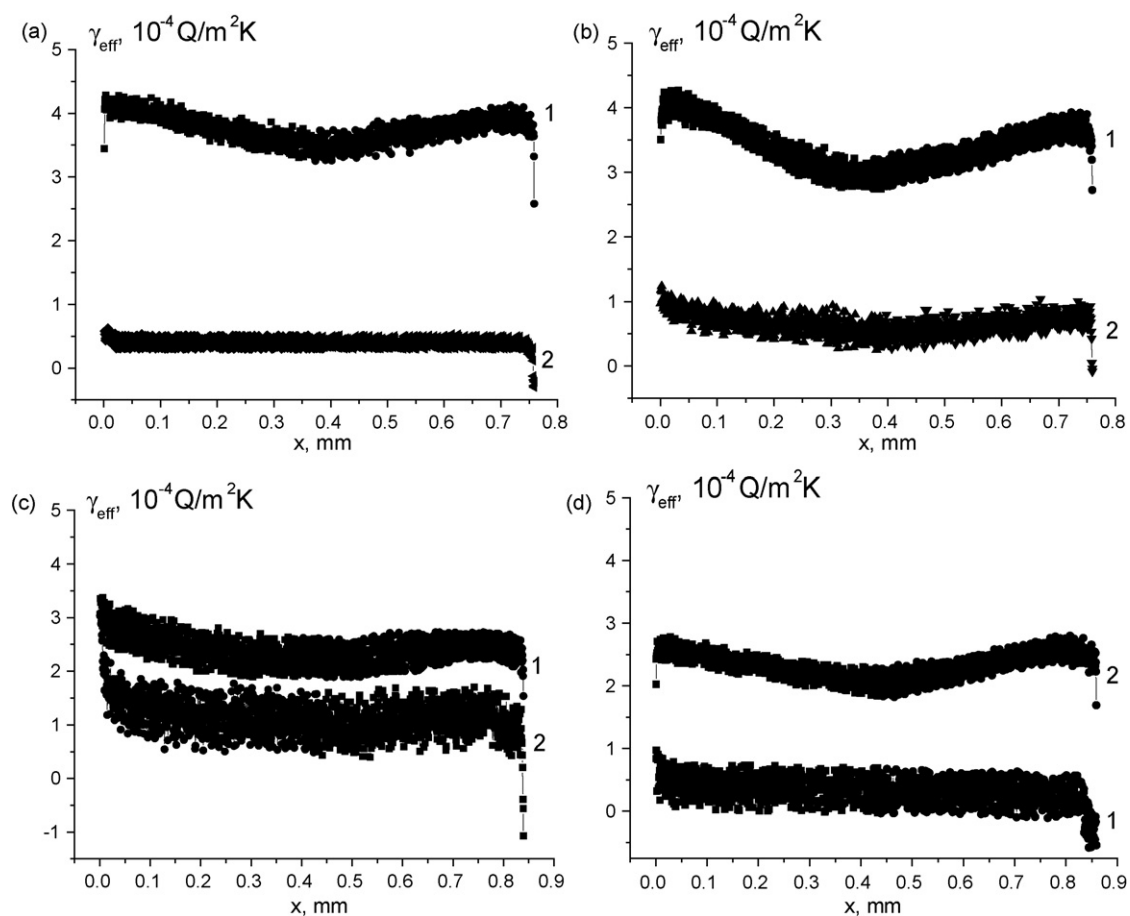


Fig. 2. Pyroelectric coefficient profile of BTS7.5 (a), BTS10 (b), BTS12.5 (c) and BTS15 (d) ceramics.

No substantial changes of the pyrocoefficient profile were observed after aging BTS7.5, BTS10 and BTS15 samples for three months at constant temperature. For BTS12.5 sample held at  $T = 27^\circ\text{C}$  in the Curie region the pyroelectric profile changed with time: a layer with inverse polarization appeared on the sample side corresponding to  $+P_s$ ; whereas a layer with increased polarization value formed on the opposite side corresponding to  $-P_s$  (Fig. 2c, curve 2). Similar profile was observed initially for BTS15 ceramics (Fig. 2d, curve 1) being in the state of poling and measurement in paraelectric phase. Like profiles are observed for BTS7.5 and BTS10 ceramics during depolarization at cooling from the paraelectric phase (Fig. 2a and b, curve 2).

It is reasonable to assume that such polarization distribution in BTS15 (Fig. 2d, curve 1) is due to its paraelectric phase state. Indeed, polarization of BTS15 sample followed by the pyroelectric profile measurement at the temperature of ferroelectric phase results in a uniform polarization distribution (Fig. 2d, curve 2).

## 5. Conclusions

The performed studies of the polarization profiles in BTS ceramics by the thermal square wave method have shown that homogeneous samples of uniform composition poled at the ferroelectric phase temperature have uniform polarization distribution. Nonuniform polarization distribution necessary for a number of applications is realized only by the depoling process resulting in a decrease of pyroelectric coefficient and ferroelectric properties. On the other hand, nonuniform polarization distribution may be obtained at room temperature in BTS ceramics with gradient composition provided the samples contain components existing at this temperature in different phases (ferroelectric and paraelectric).

## Acknowledgments

This work was supported by Grant 08-02-97502-r.center\_a of the Russian Foundation Fundamental Research and Grant

RNP 2.1.1.3674 of the Ministry of Education and Science of the Russian Federation.

## References

1. Lang, S. B. and Das-Gupta, D. K., A technique for determining the polarization distribution in thin polymer electrets using periodic heating. *Ferroelectrics*, 1981, **39**, 1249–1252.
2. Lang, S. B. and Das-Gupta, D. K., Laser intensity modulation method: a technique for determination of spatial distributions of polarization and space charge in polymer electrets. *J. Appl. Phys.*, 1986, **59**, 2151–2160.
3. Ploss, B., Emmerich, R. and Bauer, S., Thermal wave probing of pyroelectric distributions in the surface region of ferroelectric materials: a new method for the analysis. *J. Appl. Phys.*, 1992, **72**(11), 5363–5370.
4. Sandner, T., Suchaneck, G., Koehler, R., Suchaneck, A. and Gerlach, G., High frequency LImm—a powerful tool for ferroelectric thin film characterization. *Integr. Ferroelectr.*, 2002, **46**, 243–257.
5. Bauer, S. and Bauer-Gogonea, S., Current practice in space charge and polarization profile measurements using thermal techniques. *IEEE Trans. Dielectr. Electr. Insul.*, 2003, **10**, 883–902.
6. Lang, S. B., Fredholm integral equation of laser intensity modulation method (LImm): solution with the polynomial regularization and L-curve methods. *J. Mater. Sci.*, 2006, **41**, 147–153.
7. Zajozs, H. I. and Grylka, A., Thermally-generated electric fields and the linear transient pyroelectric response. *Infrared Phys.*, 1983, **23**, 271–276.
8. Carslaw, H. S. and Jaeger, J. C., *Conduction of Heat in Solids*. Clarendon Publishers, Oxford, 1959.
9. Landau, L. D. and Lifshits, E. M., *Mechanics of Continua*. Technic-Theory Lit. Publishers, Moscow, Russia, 1953.
10. Telegin, A. S., Shvydkij, V. S. and Yaroshenko, Yu. G., *Heat–Mass Transfer*. Akademkniga Publishers, Moscow, Russia, 2002.
11. Logan, R. M. and McLean, T. P., Analysis of thermal spread in a pyroelectric imaging system. *Infrared Phys.*, 1973, **3**, 15–24.
12. Lukanin, V. N., Shatrov, M. G. and Kamfer, G. M., *Teplotekhnika*. Vysshaja shkola, Moscow, Russia, 2005.
13. Malyshkina, O. V., Movchikova, A. A. and Suchaneck, G., New method for the determination of the pyroelectric current spatial distribution in ferroelectric materials. *Phys. Solid State*, 2007, **49**, 2144–2147.
14. Yasuda, N., Ohwa, H. and Asano, S., Dielectric properties and phase transitions of  $\text{Ba}(\text{Ti}_{1-x}\text{Sn}_x)\text{O}_3$  solid solution. *Jpn. J. Appl. Phys.*, 1996, **35**, 5099–5103.